Progress In Electromagnetics Research Letters, Vol. 113, 81–90, 2023

Complex Magnetic Permeability Evaluation of Steel Fibers Using Eddy Current NDE and Inverse Problem Methods

L. Gherdaoui[1, *], S. Bensaid[1], D. Trichet[2], H. Houassine[3], and N. Saoudi[4]

Abstract—This paper presents a simple approach for evaluating the complex magnetic permeability of the steel fibers used in concrete according to frequency. The approach utilises the eddy current non-destructive evaluation method, where the electrical impedance is measured using a precision LCR meter and computed using a magneto-harmonic model solved in Py-FEMM software. Initially, the electrical conductivity of the steel fiber is measured using a two-contact DC method. Then, the inverse problem method is applied to identify the complex magnetic permeability. This is achieved by iteratively minimising the difference between the calculated and measured impedances using a simplex optimization algorithm. The proposed approach offers a non-contact, non-destructive, fast, and efficient procedure to evaluate the complex permeability. The obtained results provide valuable insights into evaluating the distribution of steel fibers in concrete.

1. INTRODUCTION

Steel Fiber-reinforced concretes (SFRCs) are used in various applications such as mining, tunnelling, dam construction, and concrete pipe [1]. Fibers added to concrete positively influence its tensile strength by limiting crack propagation [2]. The toughness of SFRC depends on the dispersion and orientation of the fibers [3, 4]. During the construction of SFRC, the spatial fiber distribution is not uniform; it has a random character in its spatial filling rate, positions, and orientations which affect the stiffness of the cement matrix [5]. Thus, it is important to accurately evaluate the spatial positions and distributions of the fibers with a non-destructive (ND) automated method.

There are several methods to evaluate the distribution and dispersion of fibers in the SFRC. One of the best-known ND methods is the x-ray computed tomography technique [6, 7], it provides a clear image of SFRC internal structure, which allows for the in-depth analysis of fibers. Another widely used method is based on image processing technique applied to the cut parts of the samples; however, it is classified as a destructive method [8]. The authors in [9] highlighted an electrical contact ND method, based on the SFRC anisotropic conductivity measurement under a DC voltage, and this method is very sensitive to test conditions such as humidity and temperature. The authors in [10] proposed another ND method based on the measurement of magnetic properties using a ferrite magnetic circuit with a concrete sample as a circuit closure yoke, which requires direct contact with the samples. All mentioned methods in the cited papers give good results; however, the characterisation of the concrete and the evaluation of the fiber distribution are global and not detailed on all the tested sample zones. The authors in [11–13] proposed an ND method based on the electromagnetic induction phenomenon, with an inductor coil

Received 8 September 2023, Accepted 29 October 2023, Scheduled 10 November 2023

* Corresponding author: Loukmane Gherdaoui (l.gherdaoui@univ-bouira.dz).

[1] Laboratoire Des Matriaux Et Du Dveloppement Durable (LM2D), Faculty of Sciences and Applied Sciences Bouira University, Algeria. [2] Nantes Université, Institut de Recherche en Énergie Électrique de Nantes Atlantique, IREENA, UR 4642, F-44600 Saint-Nazaire, France. [3] Laboratoire d'Ingénierie des Systèmes Electriques et Automatiques, LISEA, Faculty of Sciences and Applied Sciences, Bouira University, Algeria. [4] Civile Engineering Department, Faculty of Sciences and Applied Sciences, Bouira University, Algeria.

supplied with AC voltage with 1 kHz frequency. The coil inductance variation allows estimating the global quantity and orientation of the fibers contained in samples. To improve the result accuracy and better understand SFRC behaviour, it is necessary to associate the electromagnetic models for analysing the spatial distributions and positions of steel fibers in the composite samples. These models can also be used to aid the design of the eddy currents ND testing setup components. The complex magnetic permeability and electrical conductivity are, therefore, the main parameters necessary to simulate these models; it is important to measure and estimate them; it is in this context that the work proposed in this article takes place.

Furthermore, the complex permeability holds significant importance in various ND testing applications, such as estimating the defects in metallic pipelines using the eddy current method [14] and detecting cracks in steel bridge [15], and it is a critical parameter in these applications, influencing the behaviour of electromagnetic fields within materials. This influence allows for precise defect detection.

The magnetic permeability value of the steel according to the frequency is nonlinear and has a complex form at high frequencies [16–18]. Okumura et al. [19] presented a contactless method for measuring the magnetic permeability of thin ferromagnetic sheets. The technique involves placing the test sample near an excitation coil, where two different coil configurations are proposed. A low-frequency (10 kHz–200 kHz) AC signal is then applied to the coil, and both inductance and resistance are measured using an LCR-meter device. The complex permeability of the sheet is calculated from the measured parameters using the electromagnetic field simulator FEKO [20]. This approach which relies on commercial simulator software is exclusively designed to determine the permeability of the single thin magnetic sheets. However, it has limitations when being applied to samples of different sizes including fiber.

Bowler [16] used a contact method to compute the complex magnetic permeability of steel plate, measuring with the 4-point alternating current potential drop (ACPD) in a range of frequency 10 Hz to 100 kHz, and the measured data are used to obtain the complex magnetic permeability using analytic model. Nevertheless, this method requires contact with the sample and is applied only on a specific size of plate, hence it cannot be used on fiber.

Several researchers [21–23] have been interested in estimating the complex magnetic permeability in the ultra-high frequency domains. These methods generally require sophisticated measuring devices.

In this paper, we present a straightforward method using eddy current non-destructive evaluation to determine the complex permeability of steel fibers utilised in concrete. Our approach features a simple experimental setup that allows measuring the impedance both with and without the presence of the fiber, effectively eliminating capacitive effects and ensuring precision through non-contact impedance measurements. It is adaptable to various sample sizes and exclusively employs open-source software for numeric calculations, enhancing accessibility for researchers. This method consists in placing the steel fiber in a container made of a solenoid coil supplied with a very low AC voltage under a frequency range of 1 kHz to 100 kHz. The measurement of the change in the real and imaginary parts of the coil impedance, with and without fiber, allows us to identify the complex magnetic permeability of the steel fiber.

Firstly, the electrical conductivity of the steel fiber is determined using the standard two-contact DC measurement. Then, the impedance of the coil with and without steel fiber is measured according to the frequency, using a 20 Hz–5 MHz precision LCR-meter. On the other hand, the inverse method involves evaluating for several times and the difference between the measured and computed impedance variation, according to the real and imaginary values of the permeability, until the satisfaction of the imposed tolerance. The impedance variation of the coil is computed, with and without fiber, for each frequency, using a magneto-harmonic model solved in Py-FEMM open source software [24]. By solving the inverse problem, the difference between the measured and computed impedance variation is minimised using a simplex algorithm provided by SCIPY optimisation libraries [25].

2. MEASUREMENT SETUP DESCRIPTION

2.1. Conductivity Measurement

In the first step, the measurement of the electrical resistance is carried out in DC using a precision digital micro ohm-meter.

Table 1. Electrical conductivity measurement.

R_{fib} (Ω)	D_{fib} (mm)	L_{fib} (mm)	L_{Afib} (mm)	σ_{fib} (MS/m)
23.53	0.54	37.76	34.96	6.487

The electrical conductivity of the fiber [S/m] (Table 1), σ_{fib}, is obtained from Ohm's law, as follows:

$$\sigma_{fib} = \frac{L_{Afib}}{R_{fib} \cdot A_{fib}} \tag{1}$$

where R_{fib}: the resistance of the steel fiber [Ohm], measured with a precision digital micro-ohm meter (Fig. 1(a)). D_{fib}: the diameter of the steel fiber [m], measured with a caliper (Fig. 1(b)). A_{fib}: the cross-section area of the steel fiber computed as: $A_{fib} = \pi \left(\frac{D_{fib}}{2}\right)^2$. L_{Afib}: the distance between the two contacts [m], representing the length of the active steel fiber (Fig. 1(d)). L_{fib}: the length of the steel fiber [m], measured with a caliper (Fig. 1(c)).

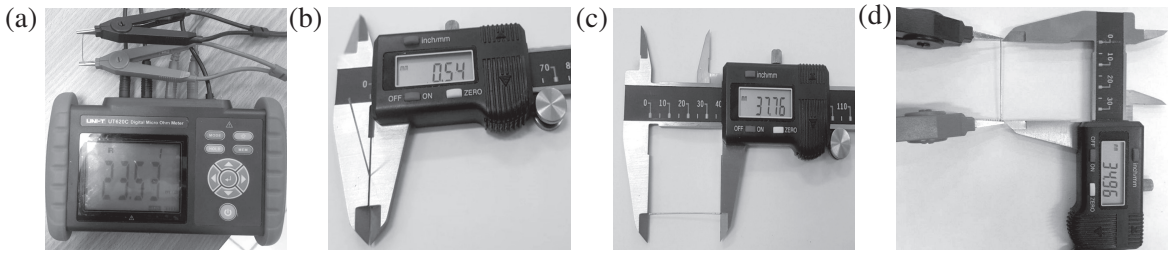

Figure 1. DC electrical resistance and geometric dimensions of the steel fiber. (a) Steel fiber resistance. (b) Steel fiber diameter. (c) Steel fiber length. (d) Steel fiber active length.

2.2. Impedance Measurement

The test bench realised for the characterisation of the steel fiber (Fig. 2) is composed of:

1- Steel fiber used in the concrete (Fig. 3(a)). It is transformed to the straight form (Fig. 3(b)) to make it easier to install into the probe.
2- LCR-meter controlled through a computer used for the measurement of the test sample impedance.
3- Eddy current probe (ECP) adapted to the dimensions of the steel fiber. It is a cylindrical PVC container wound with N_{turns} turns, making it easy to install the fiber. The ECP can be updated to adapt any size of material with characteristics given in Table 2.

Table 2. Eddy current probe dimensions.

Copper diameter (d_{co})	0.25 mm
Probe Inner diameter (d_{in})	3.00 mm
Probe length (L_p)	15.4 mm
PVC container length (L_{PVC})	37.76 mm
Number of Probe turns (N_{turns})	50

The impedance measurement of the test sample placed in the eddy current probe (Fig. 2) is carried out using the LCR-meter, which supplies the coil with a sinusoidal low voltage of amplitude 1V for each frequency in a range of 1 kHz–100 kHz.

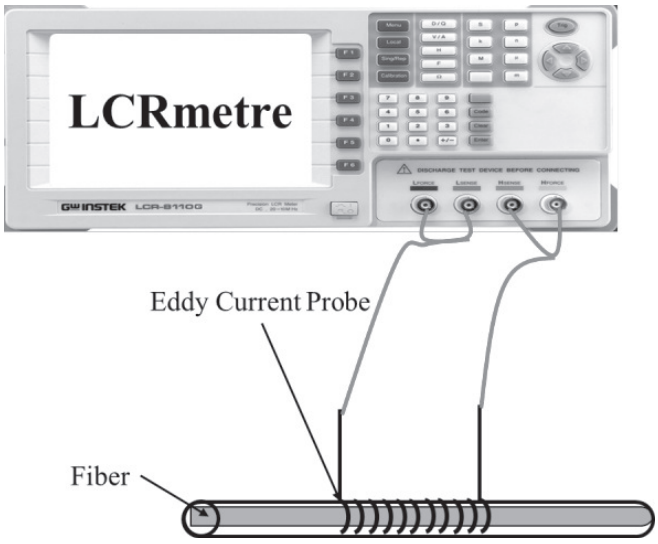

Figure 2. Impedance measurement — Experimental setup.

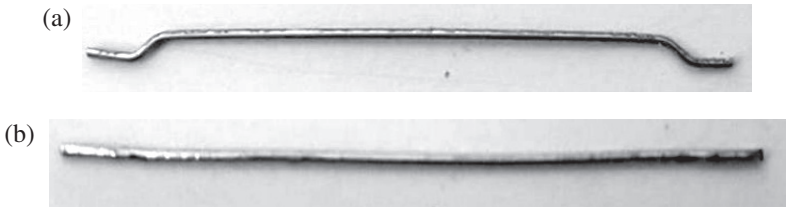

Figure 3. Straightening the steel fiber. (a) Hook end steel fiber. (b) Straight end steel fiber.

This measurement is performed both with and without the steel fiber to obtain the impedance variation.

As shown in Fig. 4, one can observe a significant variation in the resistance and reactance of the ECP in the presence of the steel fiber. This change increases with frequency. Additionally, one also observe that the variation in resistance is greater than the reactance.

3. MODEL FORMULATION — IMPEDANCE COMPUTATION

The magneto-harmonic formulation of the ECP with fiber is given in (Eq. (2)), and it is solved by the finite element method using the FEMM software [26, 27] in two dimensions. The system is represented in an axisymmetric geometric as illustrated in Fig. 5

$$\iint_{\Omega} -\frac{\partial}{\partial r}\left(\frac{1}{r\overline{\mu}}\frac{\partial A'}{\partial r}\right) - \frac{\partial}{\partial z}\left(\frac{1}{r\overline{\mu}}\frac{\partial A'}{\partial z}\right) + j\frac{\sigma_{fib}\,\omega}{r}A' = J_s \tag{2}$$

with A', $\overline{\mu}$, J_s, σ_{fib} denoting respectively $A'(0, r\mathrm{A}\varphi, 0)$ the modified magnetic vector potential, the complex magnetic permeability of the steel fiber, the source current density, and the electrical conductivity of the fiber, where $\mathrm{A}\varphi$ is the azimuth cylindric coordinate of the magnetic vector potential.

After calculating the modified magnetic vector potential, the variations of the resistance and reactance are computed using the following expression:

$$\delta R_{\mathrm{cal}} = -2 \cdot \pi \cdot \omega \cdot N_{\mathrm{turns}} \cdot \mathrm{Im}\left(\mathrm{mean}\left(\mathrm{A}'\right)\right) \tag{3}$$

$$X_{\mathrm{cal}} = 2 \cdot \pi \cdot \omega \cdot N_{\mathrm{turns}} \cdot \mathrm{Re}\left(\ \mathrm{mean}\ \left(\mathrm{A}'\right)\right) \tag{4}$$

with R_{cal}, X_{cal}, N_{turns}, ω, Re, and Im denoting respectively the calculated resistance, calculated reactance, ECP turns, electrical pulsation, real part, and imaginary part.

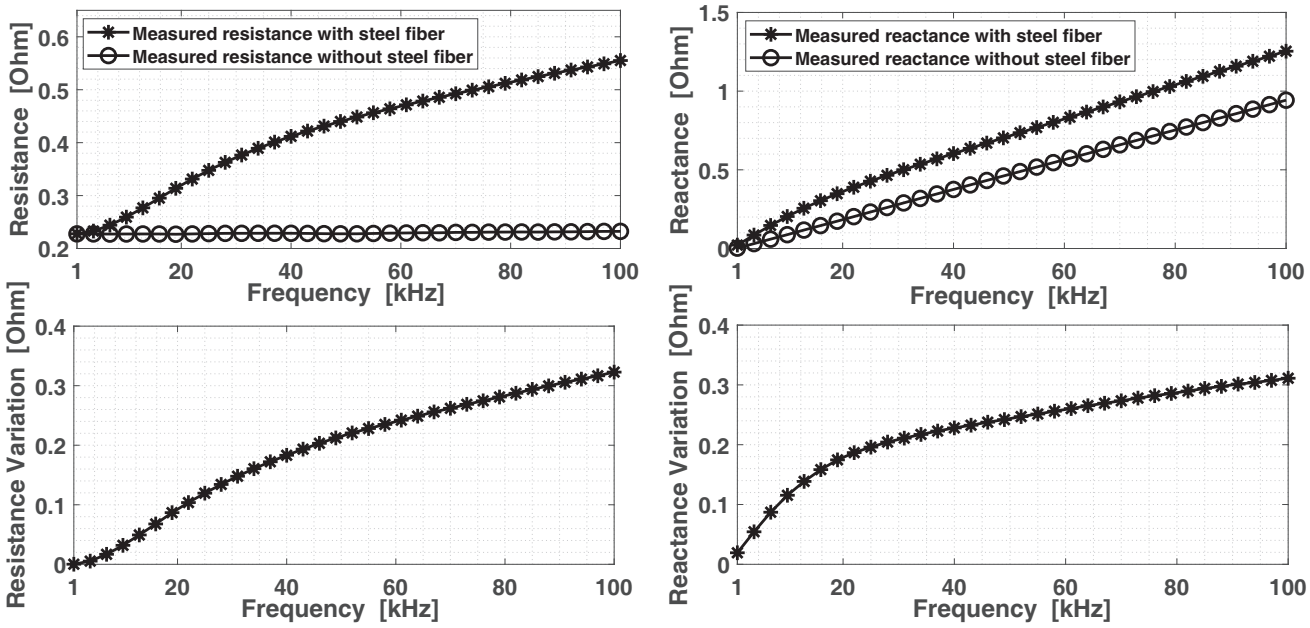

Figure 4. Impedance and impedance variation of ECP with and without the steel fiber according to frequency.

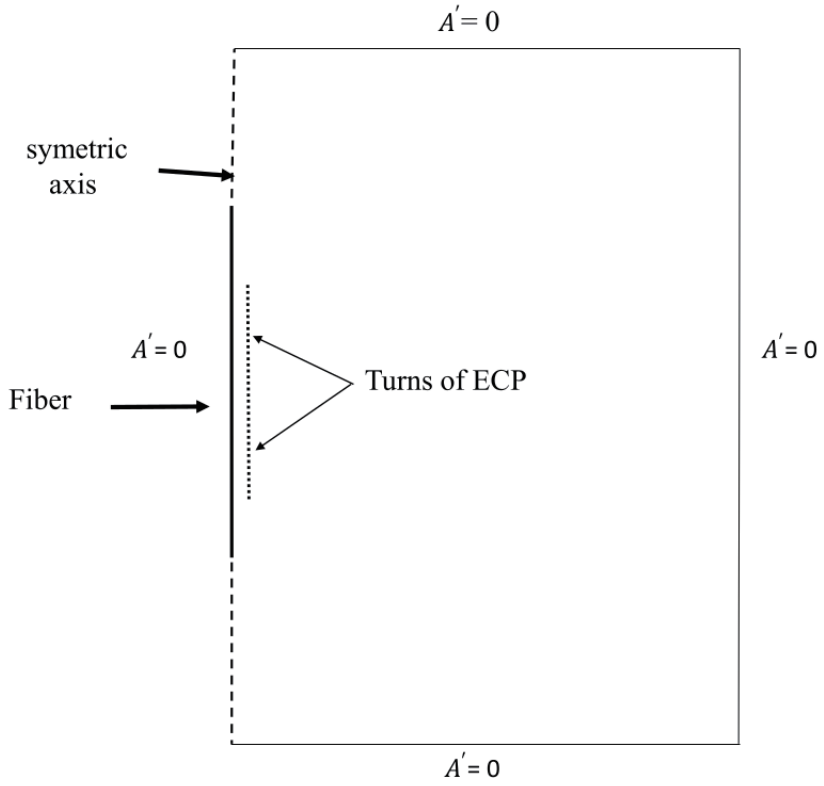

Figure 5. Geometry of the solved problem.

4. INVERSION METHOD — COMPLEX MAGNETIC PERMEABILITY IDENTIFICATION

To determine the complex magnetic permeability of steel fiber from the measurement data, an inversion method [28, 29] is required (Fig. 6).

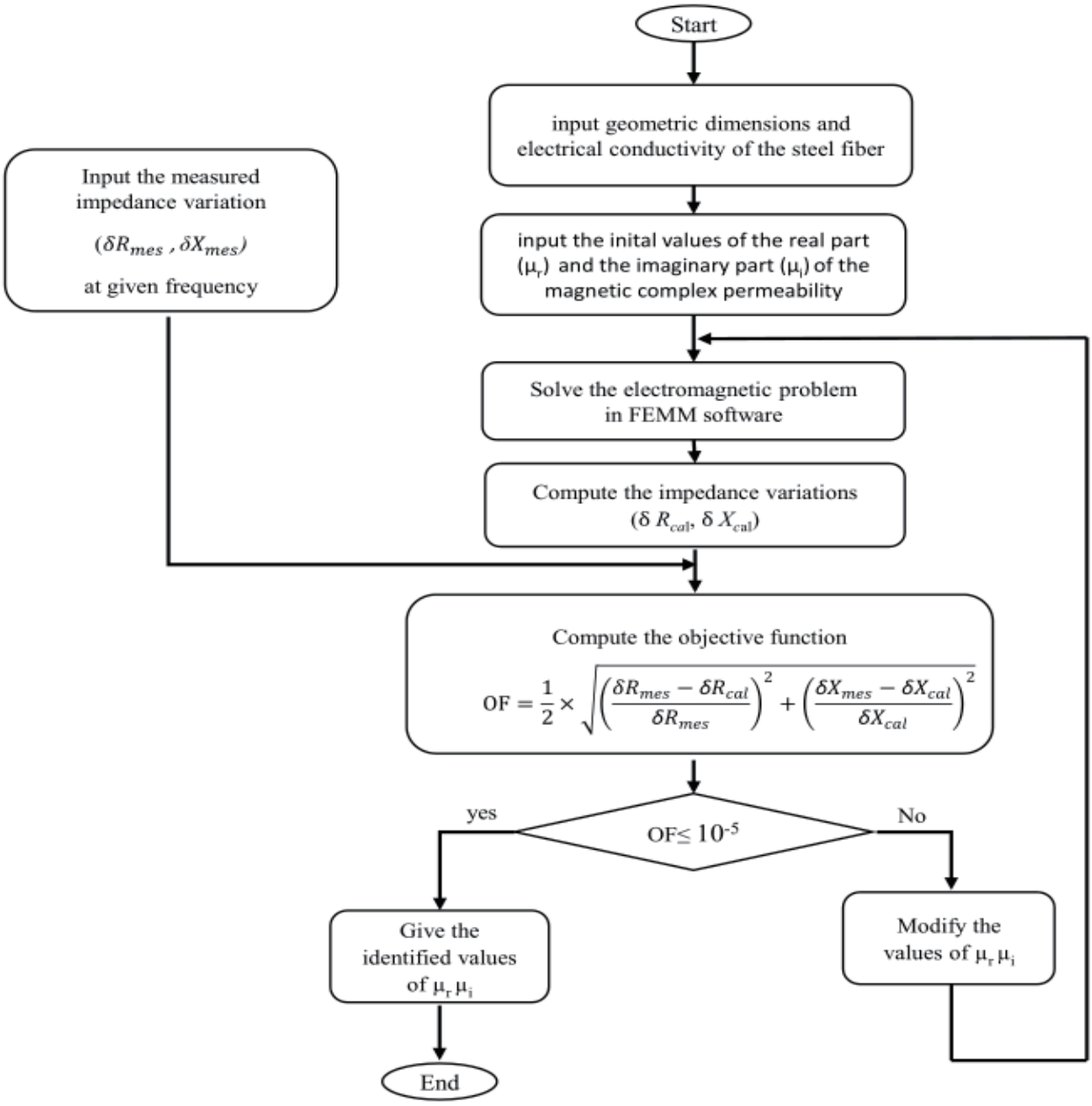

Figure 6. Inversion algorithm flowchart.

Initially, the resistance and reactance of the test sample are measured at a given frequency as explained in Section 2. Then, the FEM model is solved after introducing the sample's geometry dimensions, electrical conductivity, and initial values of the sample's real and imaginary complex magnetic permeabilities. The solution of the model is exploited to compute the resistance and reactance variations of the test sample.

The difference between the computed impedance variations and the measured one is calculated. If the difference exceeds the imposed tolerance value (10^{-5}), the values of the real and imaginary parts of complex magnetic permeability are modified. This refinement process is repeated iteratively until the difference becomes less than the tolerance using the simplex optimisation method.

For the first frequency of 1 kHz, the initial values of the real part and imaginary part of the relative permeability are set to 1 and 0.1, respectively. After performing the identification process, the identified values of the complex magnetic permeability at 1 kHz are then used as the initial values for the next frequency, which is 2 kHz. The same inversion method is applied, and the process continues iteratively for each subsequent frequency, up to a frequency of 100 kHz.

The difference between the computed impedance and the measured one is given by the following objective function (OF):

$$\mathrm{OF} = \frac{1}{2}\sqrt{\left(\frac{\delta R_{mes} - \delta R_{cal}}{\delta R_{mes}}\right)^2 + \left(\frac{\delta X_{mes} - \delta X_{cal}}{\delta X_{cal}}\right)^2} \tag{5}$$

δR_{mes}: ECP resistance variation obtained from the difference between the measured resistances (LCR-meter) with and without the presence of the steel fiber.

δR_{cal}: ECP resistance variation obtained from the difference between the computed resistances (FEMM model) with and without the presence of the steel fiber.

δX_{mes}: ECP reactance variation obtained from the difference between the measured reactances (LCR-meter) with and without the presence of the steel fiber.

δX_{cal}: ECP reactance variation obtained from the difference between the computed reactances (FEMM model) with and without the presence of the steel fiber.

The inverse method is implemented in Python, with importing the 2D finite element model PYFEMM and SCIPY optimisation libraries.

Figure 7 gives an example of the convergence process of the simplex optimisation method for searching the desired values of complex magnetic permeability at the frequency of 10 kHz. As one can see, the convergence is reached after 50 iterations to become the evaluated objective function less than the tolerance (10^{-5}). The resulting real part of the complex permeability is determined to be 56, while the imaginary part is identified as 7.9.

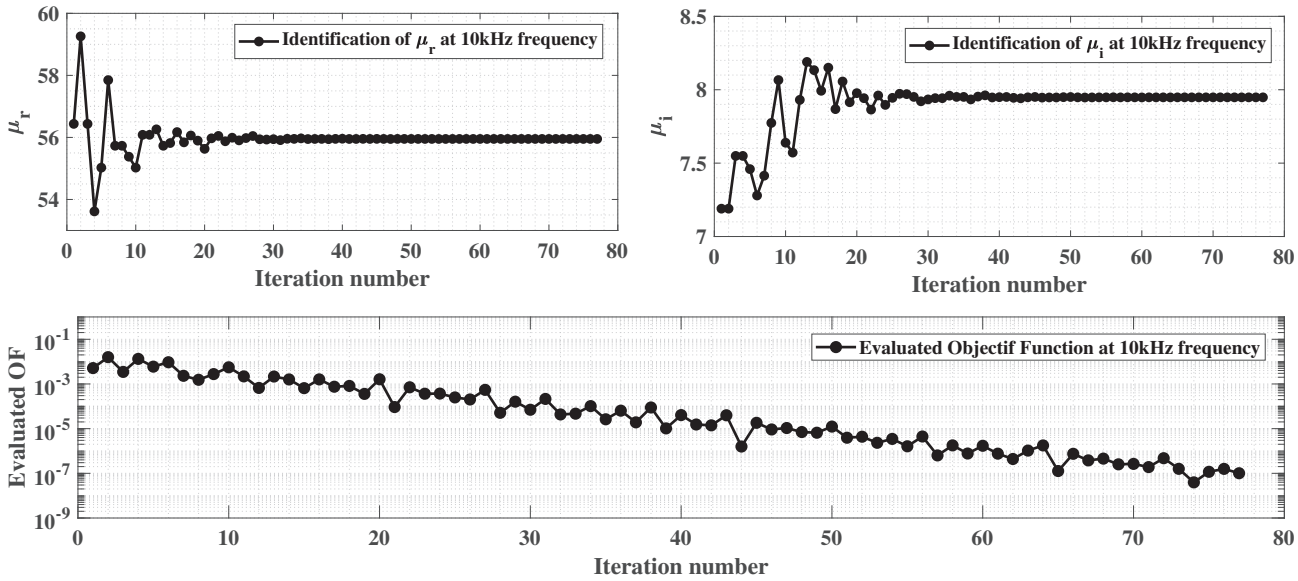

Figure 7. Identified relative permeability values with objective function tolerance at 10 kHz.

5. RESULTS AND DISCUSSION

Figure 8 shows the real part and imaginary part of relative permeability of steel fiber, according to frequency, and as shown, the real part shows a pattern of initially remaining constant, then gradually decreasing. The imaginary part exhibits a bell shape curve, which is a result of its representation of losses caused by the movement of magnetic domains. At low frequencies, these movements do occur but are relatively weak, resulting in minimal losses. Conversely, at high frequencies, the magnetic moments are no longer able to follow the field; therefore, there are no more losses.

The curve shapes of relative permeability obtained in Fig. 8 are similar to those of previous studies [15, 18, 19]. Additionally, the real part values of the complex permeability obtained closely align with the findings in previous research [30].

In order to validate the proposed method, the obtained values of the complex magnetic permeability are introduced in the direct model to compute the impedance values at each frequency. As shown in

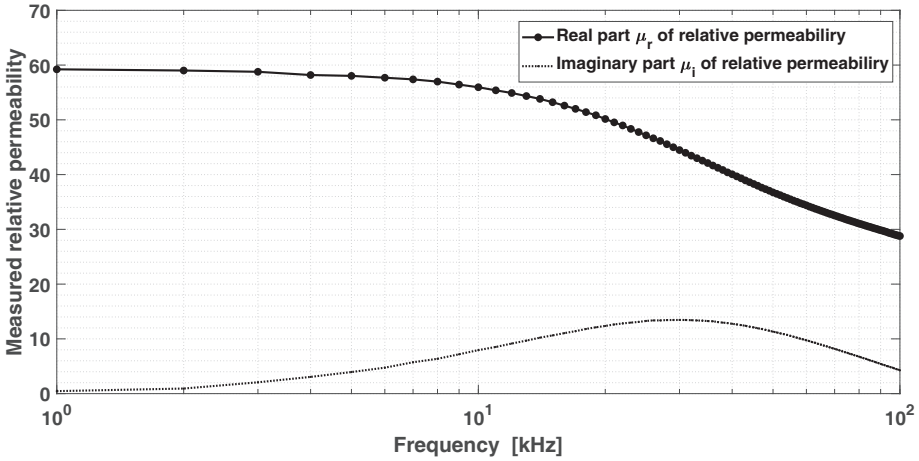

Figure 8. Magnetic relative permeability according to frequency.

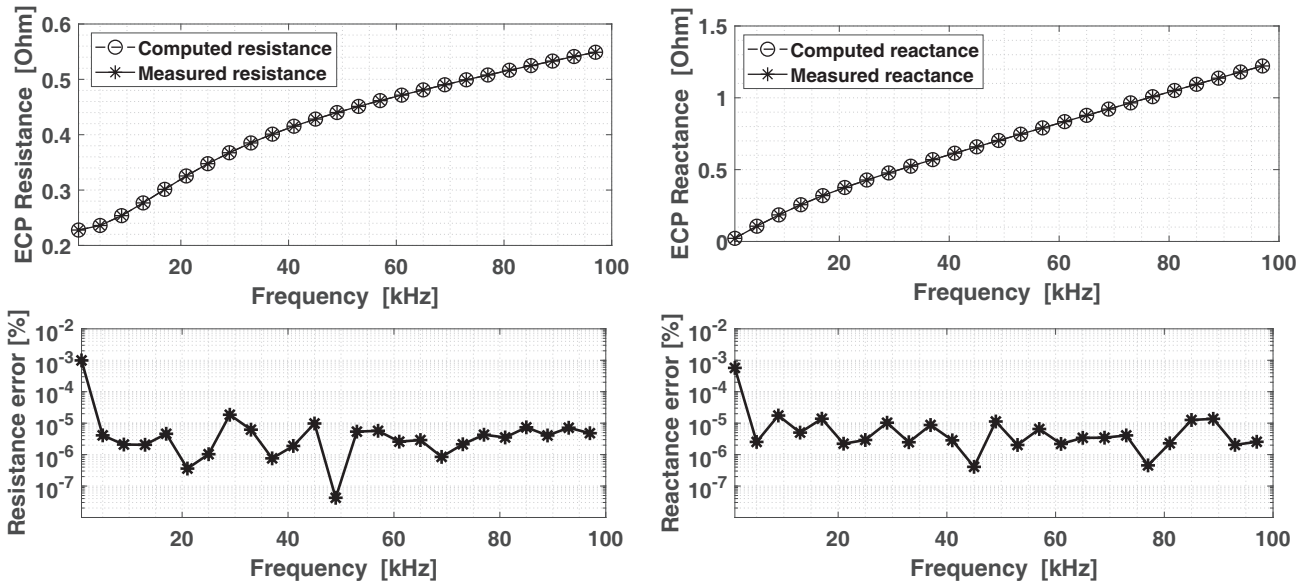

Figure 9. Computed and measured ECP impedances in the presence of the steel fiber with resistance and reactance errors according to frequency.

Fig. 9, the calculated values of the reactance and resistance match well with the measured ones. The accuracy of the proposed approach is evident, as the computed resistance error (the difference between the measured and computed resistances) is found to be less than $10^{-3}\%$ on average of 10^{-5}. Similarly, the computed reactance error (the difference between the measured and computed reactances) is also less than $10^{-3}\%$ on average of 10^{-5}. The results indicate an excellent agreement between the computed and measured impedance values, highlighting the precision of the proposed method.

6. CONCLUSIONS

This paper proposes a practical and efficient approach for evaluating the complex magnetic permeability of steel fibers according to frequency. The approach utilises the eddy current non-destructive evaluation method with a specifically designed probe combined with the inverse problem method. The eddy current probe impedance variation is measured using a precision LCR-meter. On the other hand, the impedance variation of the ECP is computed using a magneto-harmonic model implemented in PY-FEMM open-source software. The complex magnetic permeability is determined by selecting the value that minimises the difference within a specified tolerance by comparing the calculated and measured impedance variation values. This approach contributes to the characterisation and evaluation of steel fiber-reinforced materials, enabling a better understanding of their electromagnetic behaviour.

REFERENCES

1. Altun, F., T. Haktanir, and K. Ari, "Effects of steel fiber addition on mechanical properties of concrete and RC beams," *Construction and Building Materials*, Vol. 21, No. 3, 654–661, 2007.
2. Lee, J. H., "Influence of concrete strength combined with fiber content in the residual flexural strengths of fiber reinforced concrete," *Composite Structures*, Vol. 168, 216–225, 2017.
3. Akkaya, Y., S. P. Shah, and B. Ankenman, "Effect of fiber dispersion on multiple cracking of cement composites," *Journal of Engineering Mechanics*, Vol. 127, No. 4, 311–316, 2001.
4. Kang, S. T. and J. K. Kim, "The relation between fiber orientation and tensile behaviour in an ultra high performance fiber reinforced cementitious composites (UHPFRCC)," *Journal of Engineering Mechanics*, Vol. 127, No. 4, 311–316, 2001.
5. Abrishambaf, A., J. A. Barros, and V. M. Cunha, "Relation between fibre distribution and post-cracking behaviour in steel fibre reinforced self-compacting concrete panels," *Cement and Concrete Research*, Vol. 51, 57–66, 2013.
6. Bordelon, A. C., J. R. Roesler, "Spatial distribution of synthetic fibers in concrete with X-ray computed tomography," *Cement and Concrete Composites*, Vol. 53, 35–43, 2014.
7. Liu, J., C. Li, J. Liu, et al., "Study on 3D spatial distribution of steel fibers in fiber reinforced cementitious composites through micro-CT technique," *Construction and Building Materials*, Vol. 48, 656–661, 2013.
8. Fladr, J., P. Bily, and I. Broukalova, "Evaluation of steel fiber distribution in concrete by computer-aided image analysis," *Compos. Mater. Eng*, Vol. 1, No. 1, 49–70, 2019.
9. Lataste, J., M. Behloul, and D. Breysse, "Characterisation of fibres distribution in a steel fibre reinforced concrete with electrical resistivity measurements," *NDT E International*, Vol. 41, No. 8, 638–647, 2008.
10. Faifer, M., R. Ottoboni, S. Toscani, et al., "Steel fiber reinforced concrete characterization based on a magnetic probe," *2010 IEEE Instrumentation and Measurement Technology Conference Proceedings*, 157–162, 2010.
11. Cavalaro, S. H. P., R. López, J. M. Torrents, et al., "Improved assessment of fibre content and orientation with inductive method in SFRC," *Materials and Structures*, Vol. 48, 1859–1873, 2015.
12. Cavalaro, S. H. P., R. López-Carreño, J. M. Torrents, et al., "Assessment of fibre content and 3D profile in cylindrical SFRC specimens," *Materials and Structures*, Vol. 49, 577–595, 2015.
13. Torrents, J. M., A. Blanco, P. Pujadas, et al., "Inductive method for assessing the amount and orientation of steel fibers in concrete," *Materials and Structures*, Vol. 45, 1577–1592, 2012.

14. Martin, L. E., A. E. Fouda, R. K. Amineh et al., "New high-definition frequency tool for tubing and multiple casing corrosion detection," *Abu Dhabi International Petroleum Exhibition and Conference, SPE*, 2017.
15. Xia, J., Z. Yuanzhou, B. Ji, et al., "An eddy current testing method based on magnetic induction intensity for detecting cracks in steel bridge decks," *Journal of Performance of Constructed Facilities*, Vol. 37, No. 3, 04023014, 2023.
16. Bowler, N., "Frequency-dependence of relative complex magnetic permeability in steel," *AIP Conference Proceedings*, Vol. 820, No. 1, 1269–1276, 2006.
17. Tokpanov, Y., V. Lebedev, and W. Pellico, "Measurements of complex magnetic permeability of soft steel at high frequencies," *Proceedings of IPAC-2012*, 2012.
18. Abeywickrama, K., T. Daszczynski, Y. Serdyuk, et al., "Determination of complex permeability of silicon steel for use in high-frequency modeling of power transformers," *IEEE Transactions on Magnetics*, Vol. 44, No. 4, 438–444, 2008.
19. Okumura, Y., K. Fujii, T. Nagaya, et al., "Simple permeability measurement of thin ferromagnetic sheets at low frequency using LCR meter," *Electrical and Electronic Engineering*, Vol. 8, No. 2, 53–58, 2018.
20. Altair, "FEKO overview," [Online] Available: http://www.feko.info/.
21. Chen, Y., X. Wang, H. Chen, et al., "Novel ultra-wide band (10 MHz-26 GHz) permeability measurements for magnetic films," *IEEE Transactions on Magnetics*, Vol. 54, No. 11, 1–4, 2018.
22. Radonić, V., N. Blaž, and L. Živanov, "Measurement of complex permeability using short coaxial line reflection method," *Acta Physica Polonica A*, Vol. 117, No. 5, 820–824, 2010.
23. Kacki, M., M. S. Rylko, J. G. Hayes, et al., "Measurement methods for high-frequency characterizations of permeability, permittivity, and core loss of Mn-Zn ferrite cores," *IEEE Transactions on Power Electronics*, Vol. 37, No. 12, 15152–15162, 2022.
24. David Meeker (2021) PyFEMM (0.1.3) Available from: https://www.femm.info/wiki/pyFEMM.
25. Nelder, J. A. and R. Mead, "A simplex method for function minimization," *The Computer Journal*, Vol. 7, No. 4, 308–313, 1965.
26. FEMM (Version 4.2) [Computer software], 2021.
27. Bensaid, S., "Global inductance computation of a multilayer circular air coil with a wire of rectangular cross section: Case of a uniform current distribution," *Progress In Electromagnetics Research M*, Vol. 102, 149–158, 2021.
28. Bensaid, S., D. Trichet, and J. Fouladgar, "Electrical conductivity identification of composite materials using a 3-D anisotropic shell element model," *IEEE Transactions on Magnetics*, Vol. 45, No. 3, 1859–1862, 2009.
29. Safer, O. A., S. Bensaid, D. Trichet, et al., "Transverse electrical resistivity evaluation of rod unidirectional carbon fiber-reinforced composite using eddy current method," *IEEE Transactions on Magnetics*, Vol. 54, No. 3, 1–4, 2018.
30. Rose, J. H., E. Uzal, and J. C. Moulder, "Magnetic permeability and eddy-current measurements," D. O. Thompson and D. E. Chimenti, (eds.), Review of *Progress in Quantitative Nondestructive Evaluation*, Springer, Boston, MA, 1995.